HOKKAIDO UNIVERSITY

Title	Passive Shimming for Magic-Angle-Spinning NMR
Author(s)	Noguchi, So; Hahn, Seungyong; Iwasa, Yukikazu
Citation	IEEE Transactions on Applied Superconductivity, 24(3), 4400904 https://doi.org/10.1109/TASC.2013.2284548
Issue Date	2014-06
Doc URL	https://hdl.handle.net/2115/56584
Rights	© 2014 IEEE. Personal use of this material is permitted. Permission from IEEE must be obtained for all other uses, in any current or future media, including reprinting/republishing this material for advertising or promotional purposes, creating new collective works, for resale or redistribution to servers or lists, or reuse of any copyrighted component of this work in other works.
Type	journal article
File Information	TAS24-3 Shimming.pdf

Hokkaido University Collection of Scholarly and Academic Papers : HUSCAP

Passive Shimming for Magic-Angle-Spinning NMR

So Noguchi, Seungyong Hahn, and Yukikazu Iwasa

***Abstract*—The superconducting dipole magnets wound with HTS wires have been developed for a magic-angle-spinning NMR. The magnetic field of the dipole magnets is tilted from z-axis. Since the highly homogeneous magnetic field is required, the magnetic field of the dipole magnets is necessarily compensated by passive and/or active shimming. However, the compensation of all the components has not been reported. Usually, due to the axial symmetry of a solenoid magnet, only z component of the magnetic field is homogenized. In this paper, all the x, y, and z components of the magnetic field generated by the superconducitng dipole magnet are compensated because of the tilt from the z-axis.**

***Index Terms*—Nuclear magnetic resonance, numerical simulation, shimming, superconducting dipole magnet.**

I. Introduction

WHEN a superconducting magnet generating highly homogeneous magnetic field, such as MRI and NMR, is designed, it is necessary to compensate a magnetic field around the center with passive and/or active shimming [1]. Passive shimming is often employed to compensate the magnetic field using some pieces of iron. Since the magnetic field homogeneity of a few PPM is required around the center of the MRI/NMR magnet, the spherical harmonics series expansion of the magnetic field is calculated on the design stage [2], [3].

Commonly, a magnet for MRI/NMR is axially symmetric. Therefore, only the *z* component of the magnetic field is considered to be compensated [4]. When the magnetic field is compensated with passive shimming, the *z* component of the magnetic moment of correction iron is also considered so that only the *z* component of the magnetic field is homogenized around the center. In recent years, some kinds of MRI/NMR magnets whose shape is axially asymmetric have been developed but generate a homogeneous magnetic field in the *z*-direction [3], [5]. The generated magnetic field is also axially asymmetric, therefore all the components of the center magnetic field have to be compensated by shimming.

In the shimming, although all the components of the magnet moment of the correction iron piece also have to be considered, the coefficients of the spherical harmonics series expansion in only the *z*-direction magnetic field is eliminated. However, recently, a newly developed MRI/NMR magnet generates a tilted magnetic field, such as a magic-angle-spinning NMR [5]. Therefore it is necessary to eliminate the coefficients of the spherical harmonics expansion of all the magnetic field components, that are generated by all the components of the magnetic moment of correction iron pieces. Consequently, we calculated the spherical harmonics coefficients of all the magnetic field components for all the magnetic moment components. That is, we derived the equations to calculate all the components of the magnetic field around the magnet center, that are generated by a correction iron piece, using the spherical harmonics series expansion for passive shimming. Using an optimization method, the passive shimming was tried for eliminating the coefficients of the spherical harmonics series expansion of all the magnetic field components for the design of the magic-angle-spinning NMR.

Manuscript received Jul 16, 2013.

S. Noguchi is with the Graduate School of Information Science and Technology, Hokkaido University, Kita 14 Nishi 9, Kita-ku, Sapporo 060-0814, Japan (phone: +81-11-706-7671; fax: +81-11-706-7671; e-mail: noguchi@ssi.ist.hokudai.ac.jp).

S. Hahn and Y. Iwasa are with the Francis Bitter Magnet Laboratry, Massachusetts Institute of Technology, 170 Albany St., Cambridge, 02139, USA.

II. Shimming Method

A. Spherical Harmonics Coefficients by Line Current

The line current $d\boldsymbol{I}$ at the point P generates the magnetic vector potential $d\boldsymbol{A}$ at the point Q as follows:

$$d\boldsymbol{A} = \mu_0 \frac{d\boldsymbol{I}}{4\pi R} \tag{1}$$

where μ_0 and R are the permeability of free space and the distance between the points P and Q. The magnetic field generated by the current $\boldsymbol{B}_{\rm c}$ is derived from

$$\boldsymbol{B}_{\rm c} = \int_l \nabla \times d\boldsymbol{A}{\rm d}l. \tag{2}$$

The spherical harmonics function gives

$$\begin{aligned}\frac{1}{R} &= \sum_{n=0}^{\infty}\sum_{m=0}^{n}\left\{\varepsilon_m \frac{(n-m)!}{(n+m)!}\frac{r^n}{r_0^{n+1}}P_n^m(\cos\alpha)\right. \\ &\quad \left.\times P_n^m(\cos\theta)\cos[m(\psi-\phi)]\right\}\end{aligned} \tag{3}$$

where ε_m, P_n^m, r, and r_0 are the Neumann factor ($\varepsilon_m = 1$ if $m = 0$, otherwise $\varepsilon_m = 2$), the associated Legendre function, the distance from the origin to the points P and Q, respectively. The angles α, θ, ψ, and ϕ are shown in Fig. 1. Consequently, substituting (1) and (3) into (2), we can derive

$$\begin{aligned}\boldsymbol{B}_{\rm c} &= \sum_{n=0}^{\infty}\sum_{m=0}^{n}[r^n P_n^m(\cos\theta) \\ &\quad \times\{\boldsymbol{C}^{\rm c}(n,m)\cos m\psi + \boldsymbol{D}^{\rm c}(n,m)\sin m\psi\}]\end{aligned} \tag{4}$$

where

$$\begin{aligned}\begin{bmatrix}\boldsymbol{C}^{\rm c}(n,m)\\ \boldsymbol{D}^{\rm c}(n,m)\end{bmatrix} &= \boldsymbol{i}_x\begin{bmatrix}C_x^{\rm c}(n,m)\\ D_x^{\rm c}(n,m)\end{bmatrix} + \boldsymbol{i}_y\begin{bmatrix}C_y^{\rm c}(n,m)\\ D_y^{\rm c}(n,m)\end{bmatrix} \\ &\quad + \boldsymbol{i}_z\begin{bmatrix}C_z^{\rm c}(n,m)\\ D_z^{\rm c}(n,m)\end{bmatrix}\end{aligned} \tag{5}$$

and $\boldsymbol{i}_x$, $\boldsymbol{i}_y$, and $\boldsymbol{i}_z$ are the unit vector in the x-, y-, and z-direction, respectively. The coefficients $C^{\rm c}$ and $D^{\rm c}$ are obtained from the numerical integration with respect to the

line current when the coil shape is axially asymmetric, such as a dipole magnet.

When the main magnet is tilted from the z-axis, the spherical harmonics coefficients can be easily transformed using the method presented in [6].

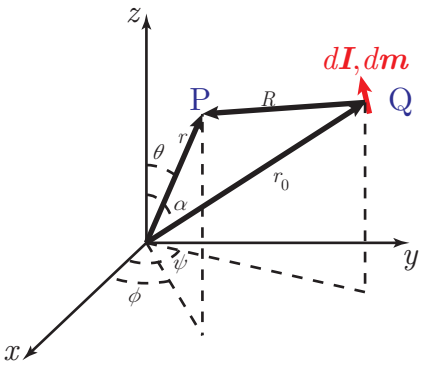

Fig. 1. Line current $d\boldsymbol{I}$ and magnetic moment $d\boldsymbol{m}$ at point Q generates magnetic vector potential $d\boldsymbol{A}$ and magnetic flux $d\Phi$ at point P.

B. Spherical Harmonics Coefficients by Magnetic Moment

The magnetic field generated $d\boldsymbol{B}_{\rm s}$ at the point P is obtained from

$$d\boldsymbol{B}_{\rm s} = -\mu_0 \nabla_{\rm P} d\Phi \tag{6}$$

where $d\Phi$ is the magnetic flux. The magnetic flux $d\Phi$ generated by the magnetic moment $d\boldsymbol{m}$ at the point Q is given by

$$d\Phi = -\frac{d\boldsymbol{m}}{4\pi\mu_0} \nabla_{\rm Q} \frac{1}{R} \tag{7}$$

Here, the dimension of the correction iron piece is given in Fig. 2. With the assumption of the constant magnetic moment $d\boldsymbol{m} = (dm_\rho, dm_\phi, dm_z)$ in cylindrical components, we can obtain the following equation from (6) and (7):

$$\boldsymbol{B}_{\rm s} = \int_{z_1}^{z_2}\int_{\rho_1}^{\rho_2}\int_{\psi_1}^{\psi_2} \frac{d\boldsymbol{m}}{4\pi} \nabla_{\rm P}\nabla_{\rm Q}\frac{1}{R} \rho {\rm d}\psi {\rm d}\rho {\rm d}z. \tag{8}$$

Consequently, substituting (3) into (8), we can derive

$$\begin{aligned} \boldsymbol{B}_{\rm s} &= \sum_{n=0}^{\infty}\sum_{m=0}^{n} [r^n P_n^m(\cos\theta) \\ &\quad \times \{\boldsymbol{C}^{\rm s}(n,m)\cos m\psi + \boldsymbol{D}^{\rm s}(n,m)\sin m\psi\}] \end{aligned} \tag{9}$$

where

$$\begin{aligned} \begin{bmatrix} \boldsymbol{C}^{\rm s}(n,m) \\ \boldsymbol{D}^{\rm s}(n,m) \end{bmatrix} &= \boldsymbol{i}_x \begin{bmatrix} C_x^{\rm s}(n,m) \\ D_x^{\rm s}(n,m) \end{bmatrix} + \boldsymbol{i}_y \begin{bmatrix} C_y^{\rm s}(n,m) \\ D_y^{\rm s}(n,m) \end{bmatrix} \\ &\quad + \boldsymbol{i}_z \begin{bmatrix} C_z^{\rm s}(n,m) \\ D_z^{\rm s}(n,m) \end{bmatrix}. \end{aligned} \tag{10}$$

The coefficients $C^{\rm s}$ and $D^{\rm s}$ are obtained from the numerical integration with respect to the volume of the correction iron piece and shown in [7].

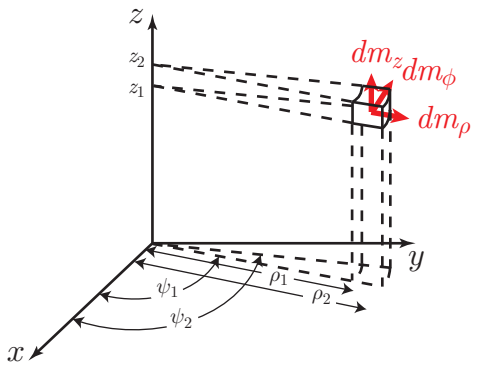

Fig. 2. Dimension of a piece of correction iron with constant magnetic moment $d\boldsymbol{m} = (dm_\rho, dm_\phi, dm_z)$ in cylindrical components.

C. Shimming Method

For homogenizing the magnetic field around the center, the coefficients $C^{\rm c}$ and $D^{\rm c}$ are compensated with the coefficients $C^{\rm s}$ and $D^{\rm s}$. That is,

$$\begin{bmatrix} \boldsymbol{C}^{\rm s}(n,m) \\ \boldsymbol{D}^{\rm s}(n,m) \end{bmatrix} + \begin{bmatrix} \boldsymbol{C}^{\rm c}(n,m) \\ \boldsymbol{D}^{\rm c}(n,m) \end{bmatrix} = \begin{bmatrix} 0 \\ 0 \end{bmatrix} \tag{11}$$

with $n \geq 1$ has to be satisfied.

In the passive shimming, the configuration of the correction iron pieces is optimized to eliminate the the coefficients $C^{\rm c}$ and $D^{\rm c}$ by adding the coefficients $C^{\rm s}$ and $D^{\rm s}$ by the micro genetic algorithm (μGA) [8]. Fig. 3 shows the flowchart of the μGA for shimming. The magnetic moment $d\boldsymbol{m}$ in the cylindrical components is computed by the magnetic moment method.

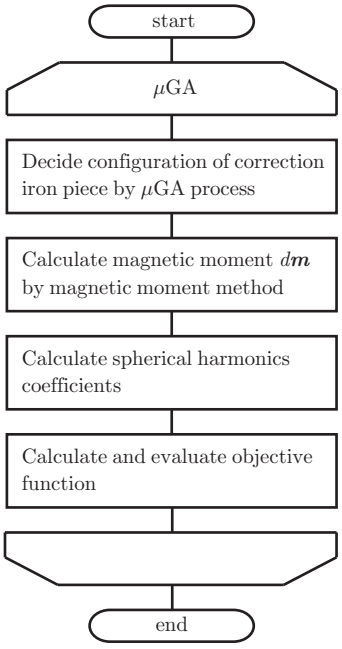

Fig. 3. Flowchart of the passive shimming computation using μGA.

III. Passive Shimming of Magic-Angle-Spinning NMR

A. Dipole Magnets and Passive Shimming

The HTS dipole magnets have been developed and manufactured for the magic-angle-spinning NMR [5]. Fig. 4 shows the schematic view of the dipole magnets. The 1.25 T magnet field generated by the HTS dipole magnet has to be tilted 54.74 deg. in y-z plane. Table I shows the spherical harmonics coefficients of the magnetic field generated by the dipole magnets, however $n \leq 4$.

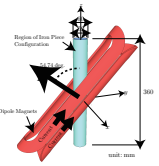

Fig. 4. Dipole magnets for magic-angle-spinning NMR. The design region of the correction iron pieces is divided into 2 (radially) × 72 (circumferentially) × 36 (height wise). The configuration of the correction iron pieces is optimized by the μGA.

TABLE I
Spherical Harmonics Coefficients of Dipole Magnets

Coefficient	x component	y component	z component
$C^{\mathrm{c}}(0,0)$	0.0	–1.02488	0.72458
$C^{\mathrm{c}}(1,0)$	0.0	0.0	0.0
$C^{\mathrm{c}}(1,1)$	0.0	0.0	0.0
$C^{\mathrm{c}}(2,0)$	0.0	2.99221	0.11988
$C^{\mathrm{c}}(2,1)$	–2.46555	0.0	0.0
$C^{\mathrm{c}}(2,2)$	0.0	–1.08113	1.02779
$C^{\mathrm{c}}(3,0)$	0.0	0.0	0.0
$C^{\mathrm{c}}(3,1)$	0.0	0.0	0.0
$C^{\mathrm{c}}(3,2)$	0.0	0.0	0.0
$C^{\mathrm{c}}(3,3)$	0.0	0.0	0.0
$C^{\mathrm{c}}(4,0)$	0.0	3010.01	–2117.02
$C^{\mathrm{c}}(4,1)$	888.047	0.0	0.0
$C^{\mathrm{c}}(4,2)$	0.0	–246.408	174.552
$C^{\mathrm{c}}(4,3)$	–190.477	0.0	0.0
$C^{\mathrm{c}}(4,4)$	0.0	54.7271	–38.6949
$D^{\mathrm{c}}(1,1)$	0.0	0.0	0.0
$D^{\mathrm{c}}(2,1)$	0.0	–1.64560	0.79069
$D^{\mathrm{c}}(2,2)$	–1.74369	0.0	0.0
$D^{\mathrm{c}}(3,1)$	0.0	0.0	0.0
$D^{\mathrm{c}}(3,2)$	0.0	0.0	0.0
$D^{\mathrm{c}}(3,3)$	0.0	0.0	0.0
$D^{\mathrm{c}}(4,1)$	0.0	–809.678	575.546
$D^{\mathrm{c}}(4,2)$	–418.947	0.0	0.0
$D^{\mathrm{c}}(4,3)$	0.0	119.083	–84.0985
$D^{\mathrm{c}}(4,4)$	74.82244	0.0	0.0

The μGA optimizes the configuration of the correction iron pieces. The design region of the correction iron pieces is subdivided into radially 2 × circumferentially 72 × heightwise 36 segmental elements. The μGA decides whether the iron piece exists in a segmental element or not, like a topology optimization [9]. The following objective function F is minimized:

$$F = \sum_{i=x,y,z} \sum_{n=1}^{4} \sum_{m=n}^{n} w(n) \{|C_i^{\mathrm{s}}(n,m) + C_i^{\mathrm{c}}(n,m)| + |D_i^{\mathrm{s}}(n,m) + D_i^{\mathrm{c}}(n,m)|\} \quad (12)$$

where $w(n)$ is a weight function of 10^{-2n}. The objective function $F = 1.275 \times 10^{-3}$ before the passive shimming.

B. Passive Shimming Result

Fig. 5 shows the optimized configuration of the correction iron pieces with the magnetization vectors. The magnetization vectors are computed by the magnetic moment and the saturated magnetic field of the magnetic field is 1.2 T. The final value of the objective function is $F = 0.410 \times 10^{-3}$. Table II shows the spherical harmonics coefficients of the correction iron pieces. Figs. 6 and 7 show the absolute value of the non-zero spherical harmonics coefficients of $n = 2$ and $n = 4$, respectively. Where as the total values of the spherical harmonics coefficients with $n = 2$ are effectively reduced as shown in Fig. 6, those with $n = 4$ are not vanished at all as shown in Fig. 7. Actually the value of $C_y(4,0)$, $C_z(4,0)$, and $D_z(4,1)$ remains largely. It is necessary to decide the weight function carefully to reduce the spherical harmonics coefficients wholly.

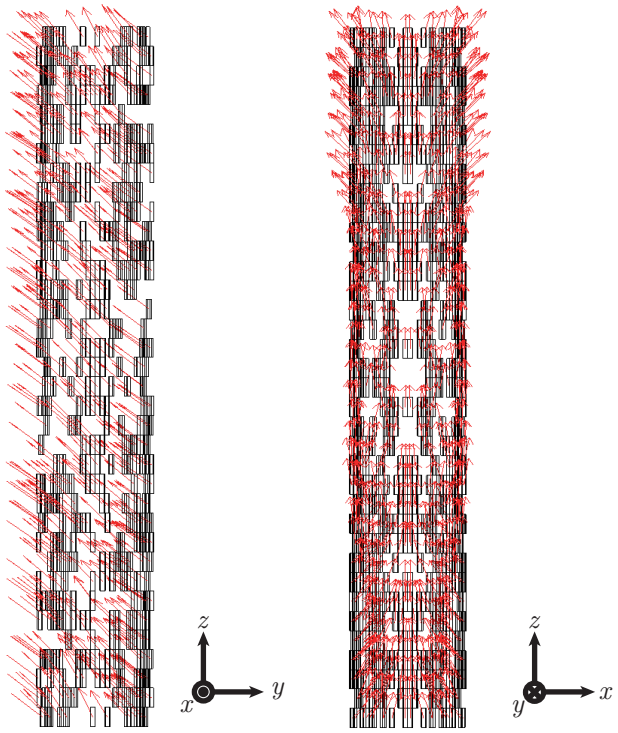

Fig. 5. The optimized configuration of the correction iron pieces with the magnetization vectors. The saturated magnetic field of the correction iron pieces is 1.2 T.

Although the coefficients of the spherical harmonics with $n = 4$ could not be reduced effectively, the homogeneity around the center is evaluated. Table III presents the inhomogeneity of the magnetic field within the sphere of 10 mm diameter. The homogeneity is enhanced by the passive shimming.

All the components of the magnetic field are simultaneously homogenized in this paper, although only z component of the magnetic field are considered hitherto. However, only the pas-

TABLE II
SPHERICAL HARMONICS COEFFICIENTS OF CORRECTION IRON PIECES

Coefficient	x component	y component	z component
$C^{\mathrm{s}}(0,0)$	0.0	–0.00064	0.00317
$C^{\mathrm{s}}(1,0)$	0.0	0.0	0.0
$C^{\mathrm{s}}(1,1)$	0.0	0.0	0.0
$C^{\mathrm{s}}(2,0)$	0.0	–2.56057	–0.12369
$C^{\mathrm{s}}(2,1)$	–2.46538	0.0	0.0
$C^{\mathrm{s}}(2,2)$	0.0	0.81339	–1.25330
$C^{\mathrm{s}}(3,0)$	0.0	0.0	0.0
$C^{\mathrm{s}}(3,1)$	0.0	0.0	0.0
$C^{\mathrm{s}}(3,2)$	0.0	0.0	0.0
$C^{\mathrm{s}}(3,3)$	0.0	0.0	0.0
$C^{\mathrm{s}}(4,0)$	0.0	5772.92	6788.71
$C^{\mathrm{s}}(4,1)$	115.135	0.0	0.0
$C^{\mathrm{s}}(4,2)$	0.0	1008.26	490.959
$C^{\mathrm{s}}(4,3)$	298.244	0.0	0.0
$C^{\mathrm{s}}(4,4)$	0.0	383.463	50.0583
$D^{\mathrm{s}}(1,1)$	0.0	0.0	0.0
$D^{\mathrm{s}}(2,1)$	0.0	1.63593	–1.70705
$D^{\mathrm{s}}(2,2)$	1.73093	0.0	0.0
$D^{\mathrm{s}}(3,1)$	0.0	0.0	0.0
$D^{\mathrm{s}}(3,2)$	0.0	0.0	0.0
$D^{\mathrm{s}}(3,3)$	0.0	0.0	0.0
$D^{\mathrm{s}}(4,1)$	0.0	–627.027	2309.17
$D^{\mathrm{s}}(4,2)$	766.329	0.0	0.0
$D^{\mathrm{s}}(4,3)$	0.0	–368.381	249.080
$D^{\mathrm{s}}(4,4)$	327.633	0.0	0.0

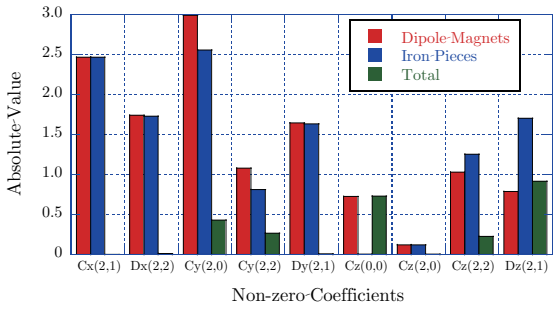

Fig. 6. The absolute value of the non-zero spherical harmonics coefficients with $n = 2$.

sive shimming does not adequately improve the homogeneity. It is necessary to combine the active shimming.

IV. CONCLUSION

We have tried to do the passive shimming to the dipole magnets for the magic-angle-spinning NMR. So far only z component of the magnetic field is homogenized, however all the components of the magnetic field are homogenized simultaneously. In the proposed passive shimming method, the spherical harmonics coefficients of all the components of the magnetic moment generated by the correction iron pieces are calculated, and the configuration of the correction iron pieces are optimized by the μGA in order to eliminate the spherical harmonics coefficients of the dipole magnets. The magnetic moment of the correction iron pieces is computed by the magnetic moment method.

Although the homogeneity of the magnetic field is improved to 35.6 ppm, it is necessary to employ the active shimming as well as the passive shimming for improving the magnetic field homogeneity more.

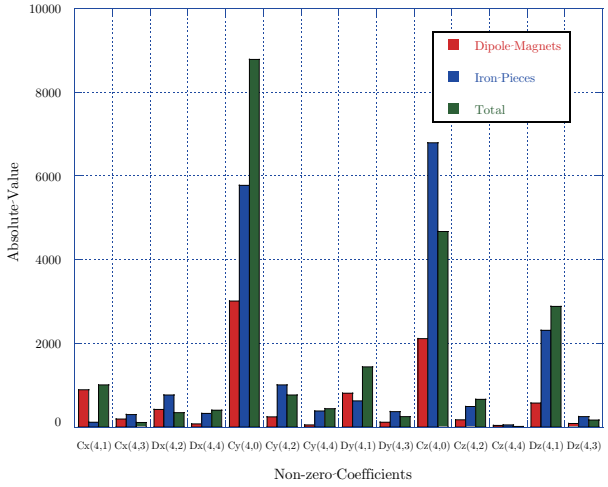

Fig. 7. The absolute value of the non-zero spherical harmonics coefficients with $n = 4$.

TABLE III
INHOMOGENEITY OF MAGNETIC FIELD WITHIN 10 MM SPHERE

	w/o shimming (ppm)	with shimming (ppm)
x component	1.1	1.2
y component	90.1	33.3
z component	62.0	12.4
All components	107.6	35.6

REFERENCES

[1] A. Belov, V. Bushuev, M. Emelianov, V. Emelianov, V. Eregin, Y. Severgin, S. Sytchevski, and V. Vasiliev, "Passive shimming of the superconducting magnet for MRI," *IEEE Trans. Appl. Supercond.*, vol. 5, no. 2, pp. 679-681, 1995.

[2] L. Feng, Z. Jianfeng, X. Lin, and S. Crozier, "A hybrid feild-harmonics approach for passive shimming design in MRI," *IEEE Trans. Appl. Supercond.*, vol. 21, no. 2, pp. 60-67, Apr. 2011.

[3] S. Kakugawa, H. Hino, A. Komura, M. Kiatmura, H. Takeshima, T. Yatsuo, and H. Tazaki, "Three-dimensional optimization of correction iron pieces for open high field MRI system," *IEEE Trans. Appl. Supercond.*, vol. 14, no. 2, pp. 1624-1627, Jun. 2004.

[4] S. Noguchi and A. Ishiyama, "An optimal design method for high-field superconducting magnets with ferromagnetic shields," *IEEE Trans. Appl. Supercond.*, vol. 7, no. 2, pp. 439-442, 1997.

[5] J. Voccio, S. Hahn, D. K. Park, J. Ling, Y. Kim, J. Bascuñán, and Y. Iwasa, "Magic-angle-spinning NMR magnet development: field analysis and prototype," *IEEE Trans. Appl. Supercond.*, vol. 23, no. 3, p. 4300804, Jun. 2013.

[6] M. A. Blanco, M. Flórez, and M. Bermejo, "Evaluation of the rotation matrices in the basis of real spherical harmonics," *Journal of Molecular Structure*, vol. 419, pp. 19-27, 1997.

[7] S. Noguchi and S. Kim, "Spherical Harmonics Coefficients of All Magnetic Field Components Generated by Iron Piece," *Proceedings of 19th International Conference on the Computation of Electromagnetic Fields*, PB5-14, 2013.

[8] Y. Watanabe, K. Watanabe, and H. Igarashi, "Optimization of meander line antenna considering coupling between nonlinear circuit and electromagnetic waves for UHF-band RFID," *IEEE Trans. Magn.*, vol. 47, no. 5, pp. 1506-1509, May 2011.

[9] Y. Tominaga, Y. Okamoto, S. Wakao, and S. Sato, "Binary-based topology optimization of magnetostatic shielding by a hybrid evolutionary algorithm combining genetic algorithm and extended compact genetic algorithm," *IEEE Trans. Magn.*, vol. 49, no. 5, pp. 2093-2096, May 2013.